



Published in final edited form as:

*Langmuir*. 2003 March 18; 19(6): 2425–2433. doi:10.1021/la0264318.

## Dielectrically Addressable Microspheres Engineered Using Self-Assembled Monolayers

Jody Vykoukal<sup>\*</sup>, Daynene Mannering Vykoukal, Susan Sharma, Frederick F. Becker, and Peter R. C. Gascoyne

The University of Texas M. D. Anderson Cancer Center, Department of Molecular Pathology, Box 089, 1515 Holcombe Boulevard, Houston, Texas 77030

### Abstract

We have used self-assembled monolayer techniques to produce a new class of microspheres with specifically engineered dielectric properties to enable their dielectrophoretic manipulation and identification in microsystems. Dielectrophoresis is an electrokinetic phenomenon that exploits frequency-dependent polarizability differences between a particle and its suspending medium to drive the movement of the particle toward or away from the high-field regions of an inhomogeneous electric field. While dielectrophoretic methods have been used extensively for cell manipulation, separation, and identification, we wished to extend the applicability of dielectrophoresis to molecular analysis by developing a panel of dielectric microspheres or “handles”. Dielectric shell theory was used to model the dielectrophoretic response for a biomimetic particle composed of a thin insulating shell over a conductive interior. We specifically sought to modulate the specific capacitance, and thereby the dielectric properties, of the particle by controlling the thickness of the insulating layer. Such a structure was fabricated by covering a gold-coated polystyrene core particle with self-assembled monolayers of alkanethiol and phospholipid. To test the prediction that the carbon chain length of these layers should dictate the dielectric properties of the particles, we constructed a panel of six microsphere types with shell compositions ranging from a C<sub>9</sub> alkanethiol monolayer to a C<sub>32</sub> hybrid bilayer membrane. These microsphere populations were distinguishable and manipulatable by dielectrophoresis in a characteristic, frequency-dependent manner as predicted by theory. Experimentally derived specific membrane capacitance values were inversely related to the insulating shell thickness and agreed with published capacitance values for planar layers of similar thicknesses. These proof of principle studies are the first to demonstrate that the dielectric properties of particles can be specifically engineered to allow their dielectrophoretic manipulation and are a first step toward the development of bead-based dielectrophoretic microsystems for multiplexed molecular separation and analysis.

### Introduction

Polymer microspheres are routinely used as labels, carriers, and solid supports for the separation and analysis of chemical, biochemical, and biological analytes. Micro-spheres conjugated with ligands, antibodies, or nucleic acid probes can be used to isolate pathogens, cell sub-populations, organelles, and RNA from a sample and to identify the presence of specific epitopes or nucleic acid sequences.<sup>1–4</sup> Analyte quantitation and microsphere identification are generally fluorescence based. Microspheres are typically manipulated in solution by means of hydrodynamic forces, as in a cytometer or other flow systems.<sup>5</sup>

Additionally, magnetophoretic forces induced by high-gradient magnetic fields are frequently employed to move and trap paramagnetic microspheres in a number of microsphere-based separation methods.<sup>6–10</sup> Here we introduce a new class of microspheres that have been specifically designed such that they can be both manipulated and identified using dielectric methods.

Dielectrophoresis (DEP) is a phenomenon in which entities of high electrical polarizability tend to move toward the high-field regions of an inhomogeneous electric field distribution and, conversely, entities of low electrical polarizability tend to be excluded from the high-field regions in the presence of a more polarizable medium.<sup>11</sup> This effect can be used to drive the movement of particles such as cells and biomolecules within a suspending medium toward or away from high-field regions in a manner dependent on the frequency of the applied electric field.<sup>11</sup> Several groups have exploited dielectric differences between different cell types to facilitate the trapping, separation, focusing, and identification of component cell populations within a mixed sample, for example.<sup>12–18</sup> In the frequency range typically used for DEP-based analysis of mammalian cell samples, cell dielectric properties are dominated by the capacitance properties of the cell membrane, which depend on membrane thickness, composition, and morphology.<sup>19,20</sup>

Dielectrophoresis is ideal for use in microfluidic microsystems, or “lab-on-a-chip” devices, particularly micro total analysis systems in which all sample preparation and analysis steps are integrated into a single device to facilitate rapid, high-throughput, low-volume molecular assays.<sup>21–24</sup> The DEP trapping of both cells<sup>12,13</sup> and molecules<sup>17,25</sup> has been shown to be straightforward. While high-discrimination dielectrophoretic analysis can be achieved for different cell types using dielectrophoretic field-flow fractionation (DEP-FFF),<sup>26</sup> for example, sequence-specific analysis of biomolecules and other macromolecular analytes by dielectrophoresis is much more challenging. This is because the dielectric properties of a particle are influenced by all polarizable entities associated with it, including the diffuse double layer of ions in the suspending medium that arises from particle surface charge.<sup>27</sup> The polarizable volume of this charge double-layer region is small compared to the volume of a large particle such as a cell. However, this double-layer volume is very large compared to the volume of a molecule and therefore dominates the dielectric properties of molecular analytes. The DEP properties of a nucleic acid molecule, for example, are dominated by the double layer associated with the charged phosphate backbone, rather than by the sequence information contained within the base pairs. This makes it impossible to employ DEP to discriminate between the minute sequence differences that are significant in typical molecular analyses.<sup>27</sup> To circumvent this limitation and thereby extend the applicability of dielectrophoresis to molecular analysis, we sought to develop a panel of different microsphere types, each having different, well-defined, or *engineered* dielectric properties and predictable dielectrophoretic behavior. By use of attached protein or nucleic acid probes to confer molecular specificity, these engineered particles could serve as dielectric “handles” for the manipulation of analytes that otherwise might not be readily discriminated on a molecular level using their intrinsic dielectric properties alone. Such microspheres would be ideally suited to micro total analysis systems because they would be amenable to selective manipulation by attractive and repulsive DEP forces provided by direct electronic control, and each particle type could be distinguished by its characteristic impedance. This is a significant advantage over magnetic particles which can only be trapped by magnetic forces or physical barriers.

In this paper, we describe the design, fabrication, and characterization of a panel of dielectric microspheres. We used a dielectric shell model<sup>28</sup> to predict the properties of microspheres having a variety of different structures and compositions, including a biomimetic thin-insulating-shell-over-conducting-interior architecture. These calculations

suggested that we could produce a panel of engineered microspheres having the desired dielectrophoretic characteristics by using a single type of conductive core particle and varying the thickness of the outer insulating layer. To produce such particles, we applied self-assembled monolayers of alkanethiols and phospholipid to gold-coated polystyrene microsphere cores. Microsphere populations having layers of different thicknesses were distinguishable and manipulatable by dielectrophoresis in a characteristic, frequency-dependent manner as predicted by the modeling studies. Analysis of the experimental DEP crossover frequency data revealed that the specific membrane capacitance of each microsphere type was related to the thickness of the insulating alkanethiol/phospholipid shell in accordance with dielectric shell theory predictions.

## Theoretical Considerations

### Dielectrophoretic Particle Manipulation

DEP is an electrokinetic phenomenon that exploits polarizability differences between particles and their suspending media to enable particle characterization and separation in spatially or temporally inhomogeneous electric fields.<sup>11</sup> Dielectrophoretic methods include conventional dielectrophoresis (cDEP), traveling wave dielectrophoresis (twDEP), and electrorotation (ROT). These can be applied to electrically manipulate, focus, disperse, trap, or levitate biological particles and macromolecules within their suspending media.<sup>12–18</sup>

For a particle that is more polarizable than its suspending medium, the cDEP force drives the particle to the high-gradient electric field region, a phenomenon known as positive dielectrophoresis. Conversely, if a particle is less polarizable than its suspending medium, the cDEP force drives the particle away from the high-gradient electric field region, a phenomenon known as negative dielectrophoresis. The conventional dielectrophoretic force,  $F_{cDEP}$ , is given by

$$F_{cDEP} = 2\pi r^3 \epsilon_m \text{Re}(f_{CM}) \nabla E^2 \quad (1)$$

where  $r$  is the particle radius,  $\epsilon_m$  is the electrical permittivity of the suspending medium, and  $\nabla E^2$  is the gradient of the applied electric field.<sup>11</sup>  $\text{Re}(f_{CM})$  is the real part of the Clausius–Mossotti factor which relates the frequency-dependent complex permittivities of the particle  $\epsilon_p^*$  and suspending medium  $\epsilon_m^*$ ,

$$f_{CM} = \frac{\epsilon_p^* - \epsilon_m^*}{\epsilon_p^* + 2\epsilon_m^*} \quad (2)$$

In the frequency range typically used for the DEP manipulation of cells and engineered microspheres, particle dispersions are dominated by the Maxwell-Wagner, or interfacial, polarization mechanism.<sup>29</sup> Polarization of charge double layers associated with particle and cell surfaces may also be exploited for dielectrophoretic manipulations. However, these surface conductance effects are most pronounced for small-diameter (5  $\mu\text{m}$  or less) particles suspended in media of very low conductivity and are usually observed at frequency extremes.<sup>30</sup> Providing the conductivity of the dielectric membrane is small,  $\epsilon_p^*$  may be approximated as

$$\epsilon_p^* = \epsilon - j \frac{\sigma}{2\pi f} \quad (3)$$

where  $\epsilon$  is the permittivity and  $\sigma$  is the conductivity of the dielectric,  $f$  is the frequency of the applied electric field, and  $j = (-1)^{1/2}$

### Modeling the Dielectrophoretic Response of an Engineered Microsphere

The dielectric properties of mammalian cells have been characterized extensively, and theoretical models for their dielectrophoretic behavior have been developed.<sup>19,30,31</sup> Dielectrically, a microsphere with the structure shown in Figure 1A mimics a mammalian cell: a spherical, conductive core (analogous to the cytoplasm) surrounded by a thin, poorly conducting shell (analogous to the plasma membrane). The dielectrophoretic responses of such engineered dielectric microspheres were modeled using dielectrophoretic shell theory (using *MATLAB*; MathWorks, Natick, MA). The complex permittivity  $\epsilon_p^*$  of microspheres such as that illustrated in Figure 1A are given by the single-shell model<sup>28,31–33</sup>

$$\epsilon_p^* = \left\{ \frac{\left(\frac{r}{r-d}\right)^3 + 2\left(\frac{\epsilon_{\text{interior}}^* - \epsilon_{\text{shell}}^*}{\epsilon_{\text{interior}}^* + 2\epsilon_{\text{shell}}^*}\right)}{\left(\frac{r}{r-d}\right)^3 - \left(\frac{\epsilon_{\text{interior}}^* - \epsilon_{\text{shell}}^*}{\epsilon_{\text{interior}}^* + 2\epsilon_{\text{shell}}^*}\right)} \right\} \quad (4)$$

where  $\epsilon_{\text{interior}}^*$  and  $\epsilon_{\text{shell}}^*$  are the complex permittivities of the interior and the insulating shell,  $r$  is the sphere radius, and  $d$  is the thickness of the insulating layer. On the basis of our experience in the dielectrophoretic manipulation of mammalian cells, we were particularly interested in the effects of modulating the specific capacitance of the insulating outer shell by changing its thickness, permittivity, or surface area. Figure 1B illustrates the cDEP frequency responses predicted for microspheres having insulating shell thicknesses between 1 and 10 nm. These responses suggest that it should be possible to engineer different types of microspheres having discrete and differentiable dielectrophoretic responses. The unique frequency response of each microsphere type would then permit dielectric indexing, whereby different microsphere types could be individually identified and manipulated. Additional simulations were performed to examine the effects of changing other structural characteristics, including the conductivity and permittivity of the microsphere core, shell, and suspending medium. To demonstrate the principle of discrete engineered microspheres, we focus here on altering shell thickness as a means of controlling the dielectrophoretic properties of the particles.

### Engineered Microsphere Design

When designing the microspheres, we sought a fabrication method that would provide a means of precisely controlling the thickness of the insulating shell that coats the microsphere core. After evaluating the properties of a variety of materials (including metals, conductive polymers, metal oxides, and insulating polymers) and a number of fabrication methods (including electroless plating, self-assembled monolayers, and thin-film methods such as physical vapor deposition and chemical vapor deposition), we decided to use gold-coated core particles and self-assembled monolayer techniques to produce microspheres with the desired structure. Dielectrically, a core consisting of a conductive shell appears identical to a solid conductive core. By use of a core particle that is primarily low-density polystyrene, the overall particle density could be greatly reduced, keeping the sedimentation force acting on the particle in aqueous suspensions reasonably small and thereby minimizing the DEP force needed to move particles that had settled. A fabrication approach utilizing self-assembled monolayers is ideally suited for this application because it permits precise control of the thickness of the outer insulating shell. The engineered microsphere depicted in Figure 2A comprises a gold-coated polymer microsphere core surrounded by a self-assembled monolayer (SAM) of alkanethiolate with an optional self-assembled outer layer of

phospholipid to form a hybrid bilayer membrane (HBM). Alkanethiols chemisorb spontaneously onto gold surfaces and self-organize into robust, densely packed monolayer films of reproducible thickness with insulating properties.<sup>34–37</sup> Plant and others have shown that well-ordered biomimetic HBMs can be formed by fusing phospholipid vesicles with alkanethiolate monolayers.<sup>38–43</sup> While these monolayer and bilayer films have been typically produced on flat, gold-coated surfaces, the microsphere design used here, and shown in Figure 2A, involves instead the fabrication of composite bilayer membranes on gold-covered microspheres. The thickness of the insulating layer surrounding the core of an engineered dielectric micro-sphere is, in principle, dependent on both the number of methylene groups in the alkyl chain of the alkanethiol SAM film and the number of methylene groups in the lipid tail of the phospholipid used to form the hybrid bilayer membrane. It should therefore be possible to produce a library of particles having insulating layers of different thicknesses and different dielectric properties (Figure 1B) by changing the length of the hydrocarbon chain in the alkanethiolate and phospholipid layers within the basic architecture depicted in Figure 2A.

## Experimental Section

### Materials

1,2-Dimyristoyl-*sn*-glycero-3-phosphocholine (DMPC, product 850345) and ganglioside GM1 (product 860065) were obtained from Avanti Polar Lipids (Alabaster, AL). The alkanethiols nonyl mercaptan ( $\text{CH}_3(\text{CH}_2)_8\text{-SH}$ , product N31400), *n*-dodecyl mercaptan ( $\text{CH}_3(\text{CH}_2)_{11}\text{-SH}$ , product 471364), and octadecyl mercaptan ( $\text{CH}_3(\text{CH}_2)_{17}\text{-SH}$ , product O1858) were obtained from Sigma-Aldrich (St. Louis, MO).

### Preparation of Engineered Microspheres

Gold-coated polystyrene microspheres manufactured by Dynal Particles AS (Oslo, Norway) were obtained from Bangs Laboratories (Fishers, IN). These beads were 9.6  $\mu\text{m}$  in diameter (coefficient of variation of <5%) and had a density of 2.2  $\text{g}/\text{cm}^3$ . The gold-coated beads were briefly washed in piranha solution (70% concentrated  $\text{H}_2\text{SO}_4$ , 30%  $\text{H}_2\text{O}_2$ ),<sup>44</sup> thoroughly rinsed with absolute ethanol, recovered by centrifugation, and dried under a stream of nitrogen. They were then combined at a concentration of 1 mg micro-sphere/mL with 1 mM nonyl, dodecyl, or octadecyl mercaptan in absolute ethanol.<sup>34–36</sup> The suspension was gently mixed for a minimum of 12 h to promote formation of the self-assembled monolayer on the microsphere surface.<sup>36</sup> The alkanethiol-coated microspheres were recovered by centrifugation, washed twice in absolute ethanol and twice in triple-distilled water, and stored at 4 °C.

Small unilamellar vesicles of either DMPC or DMPC/GM1 were prepared as follows. A 1 mg/mL solution of phospholipid in chloroform was dried under a stream of nitrogen to yield a thin film and then placed under a vacuum overnight to remove residual solvent. Solutions containing both DMPC and ganglioside GM1 (in a 20:1 mol/mol ratio) in chloroform were mixed at room temperature for an hour before the lipid was dried as described above. The dried lipid was resuspended at a concentration of 1 mg/mL in 50 mM MKPi (pH 7), 150 mM NaCl buffer with vortexing to form a suspension of large multilamellar vesicles. This vesicle solution was then subjected to bath sonication under  $\text{N}_2$  for several minutes to produce small (approximately 20–100 nm) unilamellar vesicles.

Alkanethiol-coated microspheres (1 mg microsphere/mL solution in buffer) were combined with the phospholipid vesicles (0.2 mg/mL final concentration) and gently mixed for 2 h at room temperature to form a hybrid bilayer membrane on the micro-sphere surface.<sup>38,45</sup> The

alkanethiol–phospholipid-coated microspheres were recovered by centrifugation, washed twice in buffer, and stored in buffer at 4 °C.

### Dielectric Characterization of Microspheres

Engineered microspheres were characterized using the dielectrophoretic crossover frequency method described previously for cells.<sup>46,47</sup> Briefly, the microspheres were suspended in an aqueous medium containing 8.5% (w/v) sucrose, 0.3% (w/v) dextrose, and phosphate-buffered saline (PBS) to adjust the electrical conductivity. As described previously, an aliquot of the bead suspension was placed in an open reservoir above an interdigitated, parallel gold-on-glass electrode array comprising 50 μm electrode traces separated by 50 μm gaps. The electrode was energized with between 1 and 10 V peak-to-peak at frequencies between 1 and 200 kHz to generate inhomogeneous fields for DEP manipulation. By observing microsphere movement (see Figure 3), it is possible to determine the direction and relative magnitude of the DEP force acting on each microsphere. The field frequency was adjusted until the net DEP force acting on the particle was neither positive nor negative. This frequency is the dielectrophoretic crossover frequency ( $f_c$ ). Measurements were repeated for aliquots of beads at conductivities between 25 and 425 μS/cm.

## Results and Discussion

### Engineered Microsphere Fabrication

Gold-coated polystyrene microspheres were washed and then coated with alkanethiolate and phospholipid self-assembling monolayers as described in the Experimental Section. Six different types of engineered dielectric microspheres (see Figure 2B) were constructed in this manner. Specifically, microspheres with a relatively thin insulating layer were made by coating the core particles with a single alkanethiolate monolayer of (i) nonyl mercaptan [ $\text{CH}_3(\text{CH}_2)_8\text{-SH}$ ] to give a  $\text{C}_9$  insulating layer, (ii) *n*-dodecyl mercaptan [ $\text{CH}_3(\text{CH}_2)_{11}\text{SH}$ ] to give a  $\text{C}_{12}$  insulating layer, or (iii) octadecyl mercaptan [ $\text{CH}_3(\text{CH}_2)_{17}\text{SH}$ ] to give a  $\text{C}_{18}$  insulating layer. Microspheres with thicker insulating layers were made by forming a second insulating monolayer of DMPC [with a tail length of  $\text{C}^{14}$ ] phospholipid over the alkanethiolate layer to form a HBM as follows: (iv) nonyl mercaptan *plus* DMPC to give a  $\text{C}_{23}$  insulating layer, (v) *n*-dodecyl mercaptan *plus* DMPC to give a  $\text{C}_{26}$  insulating layer, or (vi) octadecyl mercaptan *plus* DMPC to give a  $\text{C}_{32}$  insulating layer.

Initial studies revealed that the engineered microspheres had a tendency to aggregate and to stick to glass surfaces. In an effort to mitigate these effects, we incorporated the sialic-acid bearing phospholipid ganglioside GM1 into the DMPC vesicles to impart a net negative charge on the microsphere surfaces (as displayed by mammalian erythrocytes<sup>48,49</sup>) and thereby reduce microsphere interaction with the glass and other microspheres. Ganglioside incorporation into the outer lipid layer of the engineered microspheres reduced sticking qualitatively without noticeably altering their DEP properties.

### Dielectric Characterization of Engineered Microspheres

We analyzed the dielectrophoretic crossover frequencies of the six different microsphere types to determine if the engineered beads possessed discrete dielectric properties as expected. The single-shell dielectric model predicts that an increase in the thickness of the insulating outer shell will result in an increase in the crossover frequency of the microsphere (Figure 1B) according to the approximate expression shown below (eq 5).<sup>50</sup> Note that this expression is valid only when the conductivity of the insulating shell is negligible:

$$C_{\text{mem}} \approx \frac{\sigma_s}{r\pi\sqrt{2}f_c} \quad (5)$$

where, also, from basic dielectric theory

$$C_{\text{mem}} = \frac{\epsilon_0\epsilon_{\text{mem}}}{d} \quad (6)$$

$C_{\text{mem}}$  is the specific membrane capacitance,  $\sigma_s$  is the conductivity of the suspending medium,  $r$  is the radius of the engineered microsphere,  $f_c$  is the crossover frequency,  $\epsilon_0$  is the permittivity of free space,  $\epsilon_{\text{mem}}$  is the permittivity of the insulating layer, and  $d$  is the thickness of the insulating layer. Equation 5 shows that the slope of a plot of  $f_c$  versus  $\sigma_s$  will be inversely proportional to the  $C_{\text{mem}}$  for a given engineered microsphere type. Combining eq 5 and eq 6 yields the relationship

$$d = \frac{f_c}{\sigma_s} (r\pi\sqrt{2}\epsilon_0\epsilon_{\text{mem}}) \quad (7)$$

indicating that the slope of a plot of  $f_c$  versus  $\sigma_s$  should increase with increasing membrane thickness.

The dielectrophoretic crossover frequency was determined for each microsphere type ( $C_9$ ,  $C_{12}$ ,  $C_{18}$ ,  $C_{23}$ ,  $C_{26}$ , and  $C_{32}$ ) in suspending media of different conductivities by adjusting the field frequency until microsphere movement reached a null. As shown in Figure 4, the dielectrophoretic properties of the engineered dielectric microspheres showed a clear dependence on the thickness of the insulating outer shell determined by the choice of alkanethiol and phospholipid carbon chain length, as predicted.

The  $y$ -intercept on the conductivity axis occurs close to zero, showing that the conductivities of the insulating layers are very low and suggesting that the self-assembled monolayers provide a robust insulating layer for which the approximation of eq 5 is valid.<sup>50</sup> These data also suggest that we have avoided any significant surface conductance effects, which would have instead been indicated by a positive  $y$ -axis intercept.<sup>30</sup> The coefficient of variance of the dielectric properties of each engineered microsphere type evident from the error bars on the crossover frequency plot far exceeded measurement errors, was the same for all of the microsphere types, and was comparable to the large variability we have previously reported in dielectrophoretic studies of mammalian cell populations which are known to be inhomogeneous.<sup>19,20,51</sup> This was surprising in light of the uniform particle size distributions generally associated with polymer microspheres (and specified by Dynal for the gold-coated beads) and the precise control of layer formation that self-assembled monolayer techniques generally afford. We thought that this distribution of dielectric properties might reflect variability in the characteristics of the microsphere core particle population, such as slight differences in surface roughness or uniformity of the gold coating. Scanning electron microscopy (SEM) analysis revealed that while the size distribution of the particles was fairly tight, the surfaces of the gold-coated polystyrene microspheres were rough and that the extent of roughness varied greatly from particle to particle. As shown in Figure 5, the microsphere surfaces appear to be stippled with multiple deposits of gold approximately 0.15–0.55  $\mu\text{m}$  in diameter. Dynal Particles AS supplies the gold-coated microspheres primarily for use in electronic applications, including conductive adhesive and microspacer applications.<sup>52</sup> Thus, the manufacturing scheme for these particles is

presumably optimized to yield uniformly sized, conductive spheres for which the extent of surface roughness is not important. For our application, however, any variability in surface roughness is detrimental because it will affect the total surface area, and thereby the capacitance properties, of the self-assembled insulating outer layers. Our studies of cells have indicated that dielectrophoresis is an exquisitely sensitive method for sensing changes in membrane capacitance associated with tumorigenesis, apoptosis, and other cellular disease states because small changes in cell membrane capacitance corresponding to alterations in membrane surface area can be detected easily.<sup>19,20</sup> In light of those findings, the variability in surface roughness, and correspondingly, in surface area, of the self-assembled insulating layers could account for the larger than expected coefficient of variance in the dielectric properties displayed by the engineered microspheres. Indeed, more careful analysis of the standard deviations of the crossover frequencies reveals approximately 20% variation within every engineered bead type we made, regardless of the thickness or composition of the outer insulating layer and regardless of the suspending medium conductivity. This variation far exceeds the random error in measuring crossover frequencies, which has been determined to be approximately 5%. This supports the conclusion that the observed variations in the dielectric properties of the engineered microspheres resulted from a consistent distribution of microsphere core structures in our stock of metallized polystyrene beads rather than from random variations in the thicknesses of the different self-assembled dielectric layers.

### Analysis of Engineered Microsphere Characteristics

To compare the characteristics of the insulating monolayer and hybrid bilayer shells surrounding the engineered microspheres with those that have been reported for planar layer systems, we chose to evaluate the crossover frequency data in terms of capacitance. We derived the specific capacitance for the insulating layers of the six microsphere types from the slopes of the dielectrophoretic crossover frequency plots using eq 5.<sup>50</sup> For preliminary analysis, we chose to present this capacitance data in a format utilized by Plant<sup>38</sup> in which the inverse specific capacitance for each microsphere type is plotted versus the number of carbons present in the alkanethiol monolayer (Figure 6). We also performed a more rigorous analysis of the dependence of the microsphere properties on the insulating shell thickness  $d$  as used more typically in DEP modeling. We estimated the thickness of the various insulating shells by using literature values for the thickness of the hydrocarbon tail of the DMPC phospholipid<sup>53</sup> (since only the hydrocarbon portion of the phospholipid layer contributes to the capacitance, we ignored the thickness of the hydrated headgroup<sup>38,54</sup>) and the thickness of the alkanethiol layers as determined by optical ellipsometry.<sup>35</sup> A plot of the inverse specific capacitance versus the estimated layer thickness in angstroms for the six engineered microsphere types is shown in Figure 7 (closed squares). The calculated thickness for the C<sub>18</sub> alkanethiol SAM was quite similar to that of the C<sub>23</sub> HBM (25.5 and 24.8 Å, respectively), explaining the coincidence of the crossover frequency plots for those microsphere types (Figure 4). We also calculated the  $C_{\text{mem}}$  for each layer using eq 6 and the total theoretical specific membrane capacitance for the engineered microspheres using the following relationship:<sup>38</sup>

$$\frac{1}{C_{\text{mem}}(\text{total})} = \frac{1}{C_{\text{mem}}(\text{alkanethiol})} + \frac{1}{C_{\text{mem}}(\text{phospholipid})} \quad (8)$$

where the permittivities ( $\epsilon_{\text{mem}}$ ) of the alkanethiol and lipid layers were taken to be 2.25<sup>40,55</sup> and 2.7,<sup>39</sup> respectively. These theoretical specific membrane capacitance values are also shown in Figure 7 (open circles).



The crossover-frequency-derived specific capacitance values are in general agreement with those observed by others for planar layers of similar thicknesses,<sup>40,41</sup> but a confounding factor in comparing the capacitance values is the difference in solvent conditions and other experimental conditions which can modify the composition and permittivity of the layers. Previous studies of alkanethiol monolayers have revealed that self-assembled monolayers composed of relatively short-chain alkanethiols ( $C_{10}$  and shorter) are less completely ordered and do not pack as well as those formed by longer chain alkanethiols, presumably because interchain van der Waals interactions are not as extensive.<sup>35,56,57</sup> In keeping with these previous observations, we noted that engineered microspheres coated with a  $C_9$  alkanethiol monolayer displayed a higher specific membrane capacitance than expected (with an observed  $C_{\text{mem}}$  of  $4.10 \mu\text{F}/\text{cm}^2$  versus a theoretical  $1.66 \mu\text{F}/\text{cm}^2$ ), indicating that the insulating shell behaved as if it were much thinner than predicted by previous measurements.<sup>35</sup> This increase in capacitance is also consistent with that observed by Lingler et al. for hybrid bilayer membranes having small coverage defects.<sup>45</sup> Comparison of the specific membrane capacitance values for engineered microspheres coated with alkanethiol monolayers versus those having hybrid bilayer membranes suggested that the addition of the phospholipid layer to the alkanethiol monolayer caused the alkanethiols to become more organized (see Figure 6). This agrees with the previous observations by Plant of hybrid bilayer membranes in a planar configuration.<sup>42</sup> The ability to detect such differences in the organization of the insulating shell of the engineered microsphere is evidence of the sensitivity of dielectrophoretic measurement techniques.

Our ability to successfully modulate the specific capacitance of the microspheres by varying the insulating layer thickness is illustrated in Figure 7. The experimental specific membrane capacitance values were determined using data from the dielectrophoretic crossover frequency studies. The theoretical  $C_{\text{mem}}$  for each microsphere type was calculated from basic capacitance theory (eq 6 and eq 8) using values for the layer thicknesses and permittivities obtained from the literature. These reported values are dependent upon solvent and experimental conditions, as well as layer morphology; thus, they may not be entirely representative of our particular system. Nevertheless, the experimental and theoretical capacitance values are in reasonable agreement.

Several groups have presented the concept of using beads in microfluidic devices to increase the total surface area available for chemical and biochemical reactions, including packing beads into microfluidic channels,<sup>3,58</sup> trapping beads at built-in physical barriers<sup>59</sup> or inside microfilter chambers,<sup>60-61</sup> and patterning functionalized beads in microfluidic devices using microcontact printing and self-assembly.<sup>62</sup> The new class of dielectrically engineered microspheres described in this paper provides functionalities that go beyond those of more conventional microspheres because the customized dielectric properties allow both microsphere manipulation and identification within a microfluidic environment. Because the specific capacitance of each microsphere type was a function of the thickness of the insulating shell, differential dielectrophoretic manipulation of the various microsphere types within a mixed suspension was possible. Furthermore, the characteristic dielectric properties of each microsphere type permit the dielectric identification and indexing of different microsphere types within a mixture by alternating current (ac) impedance spectroscopy (data not shown). Our studies therefore provide a proof of principle demonstration that the dielectric properties of microspheres can be specifically engineered to yield particles that can be selectively and differentially trapped, released, moved, and identified in microfluidic devices using dielectrophoretic forces. The self-assembled, biomimetic surface of these engineered microspheres could be functionalized with nucleic acid or antibody probes using established methods<sup>63-65</sup> to enable the development of a dielectrophoresis-based microsystem for multiplexed molecular separation and analysis. Using mixture theory, we calculate that the binding of analyte molecules to an engineered microsphere at a surface

coverage of 10% yields only a 3% change in the microsphere crossover frequency, assuming  $\epsilon_{\text{analyte}} = 2\epsilon_{\text{mem}}$  and an analyte diameter similar to the thickness of the bilayer. This indicates that at typical binding densities, the dielectric properties of engineered microspheres should be essentially independent of analyte binding. Therefore, a mixture of appropriately functionalized dielectric microsphere types could be used to simultaneously assay a sample for multiple analytes. Quantitation of the captured analytes by secondary fluorescent labeling could be correlated with simultaneous impedance spectroscopy to identify the microsphere type and therefore yield multiplex analysis capabilities. Finally, methods such as dielectrophoretic field-flow fractionation could be used to isolate multiple analytes from a mixture for additional characterization, if required, using different dielectrically engineered microspheres as handles for the various target species.

## Conclusions

The aim of this study was to design and produce microspheres with calculable dielectric properties and predictable dielectrophoretic behavior for use as mobile components in dielectrophoresis-based microsystems for molecular analysis. Insulating self-assembled monolayers of alkanethiols and phospholipid were formed on conductive gold-coated core particles to produce a panel of microsphere types with different shell thicknesses. As predicted, the dielectrophoretic crossover frequencies and the specific membrane capacitances of the microspheres could be modulated by varying the thickness of this insulating layer. Because these engineered dielectric microspheres are both identifiable and differentially manipulatable, they should extend multiplexed molecular assay and isolation capabilities to dielectrophoresis-based microfluidic devices.

## Acknowledgments

This work was supported by DARPA under Contract N66001-97-C-8608 and Grant Agreement DAAD19-00-1-0515 from the Army Research Office and by National Cancer Institute Award 4R33 CA 88364-2. We also acknowledge Cancer Center Core Grant CA16672 and Kenneth Dunner, Jr., at the M. D. Anderson Cancer Center High Resolution Electron Microscopy Facility.

## References

1. Carson RT, Vignali DA. *J. Immunol. Methods* 1999;227:41. [PubMed: 10485253]
2. Iannone MA, Taylor JD, Chen J, Li MS, Rivers P, Slentz-Kesler KA, Weiner MP. *Cytometry* 2000;39:131. [PubMed: 10679731]
3. Ohmura N, Lackie SJ, Saiki H. *Anal. Chem* 2001;73:3392. [PubMed: 11476240]
4. Christodoulides N, Tran M, Floriano PN, Rodriguez M, Goodey A, Ali M, Neikirk D, McDevitt JT. *Anal. Chem* 2002;74:3030. [PubMed: 12141661]
5. Watson JV. *Cytometry* 1999;38:2. [PubMed: 10088971]
6. Miltenyi S, Muller W, Weichel W, Radbruch A. *Cytometry* 1990;11:231. [PubMed: 1690625]
7. Radbruch A, Mechtold B, Thiel A, Miltenyi S, Pfluger E. *Methods Cell Biol* 1994;42:387. [PubMed: 7533249]
8. Deng T, Whitesides GM, Radhakrishnan M, Zabow G, Prentiss M. *Appl. Phys. Lett* 2001;78:1775.
9. Deng T, Prentiss M, Whitesides GM. *Appl. Phys. Lett* 2002;80:461.
10. Choi J-W, Oh KW, Thomas JH, Heineman WR, Halsall HB, Nevin JH, Helmicki AJ, Henderson HT, Ahn CH. *Lab on a Chip* 2002;2:27. [PubMed: 15100857]
11. Pohl, HA. *Dielectrophoresis: The Behavior of Neutral Matter in Nonuniform Electric Fields*. London: Cambridge University Press; 1978.
12. Becker FF, Wang XB, Huang Y, Pethig R, Vykoukal J, Gascoyne PRC. *Proc. Natl. Acad. Sci. U.S.A* 1995;92:860. [PubMed: 7846067]
13. Wang XB, Huang Y, Burt JPH, Markx GH, Pethig R. *J. Phys. D* 1993;26:1278.

14. Morgan H, Hughes MP, Green NG. *Biophys. J* 1999;77:516. [PubMed: 10388776]
15. Brown AP, Betts WB, Harrison AB, O'Neill JG. *Biosens. Bioelectron* 1999;14:341. [PubMed: 10230035]
16. Arnold WM. *IEEE Trans. Ind. Appl* 2001;37:1468.
17. Washizu M, Suzuki S, Kurosawa O, Nishizaka T, Shinohara T. *IEEE Trans. Ind. Appl* 1994;30:835.
18. Kaler KV, Jones TB. *Biophys. J* 1990;57:173. [PubMed: 2317544]
19. Wang XB, Huang Y, Gascoyne PRC, Becker FF, Hoelzel R, Pethig R. *Biochim. Biophys. Acta* 1994;1193:330. [PubMed: 8054355]
20. Huang Y, Wang XB, Becker FF, Gascoyne PRC. *Biochim. Biophys. Acta* 1996;1282:76. [PubMed: 8679663]
21. van den Berg, A.; Olthuis, W.; Berveld, P., editors. *Micro Total Analysis Systems* 2000. Dordrecht: Kluwer Academic; 2000.
22. van den Berg, A.; Ramsey, JM., editors. *Micro Total Analysis Systems* 2001. Dordrecht: Kluwer Academic; 2001.
23. Reyes DR, Iossifidis D, Auroux PA, Manz A. *Anal. Chem* 2002;74:2623. [PubMed: 12090653]
24. Auroux PA, Iossifidis D, Reyes DR, Manz A. *Anal. Chem* 2002;74:2637. [PubMed: 12090654]
25. Washizu M, Kurosawa O. *IEEE Trans. Ind. Appl* 1990;26:1165.
26. Wang XB, Yang J, Huang Y, Vykoukal J, Becker FF, Gascoyne PRC. *Anal. Chem* 2000;72:832. [PubMed: 10701270]
27. Gascoyne PRC, Vykoukal J. *Electrophoresis* 2002;23:1973. [PubMed: 12210248]
28. Irimajiri A, Hanai T, Inouye A. *J. Theor. Biol* 1979;78:251. [PubMed: 573830]
29. von Hippel, A. *Dielectrics and Waves*. Boston: Artech House; 1995.
30. Arnold WM, Schwan HP, Zimmermann U. *J. Phys. Chem* 1987;91:5093.
31. Marszalek P, Zielinsky JJ, Fikus M, Tsong TY. *Biophys. J* 1991;59:982. [PubMed: 1831052]
32. Turcu I, Lucaciu CM. *J. Phys. A* 1989;22:985.
33. Kakutani T, Shibatani S, Sugai M. *Bioelectrochem. Bioenerg* 1993;31:131.
34. Nuzzo RG, Allara DL. *J. Am. Chem. Soc* 1983;105:4481.
35. Porter MD, Bright TB, Allara DL, Chidsey CED. *J. Am. Chem. Soc* 1987;109:3559.
36. Bain CD, Troughton EB, Tao Y-T, Evall J, Whitesides GM, Nuzzo RG. *J. Am. Chem. Soc* 1989;111:321.
37. Ulman A. *Chem. Rev* 1996;96:1533. [PubMed: 11848802]
38. Plant AL. *Langmuir* 1993;9:2764.
39. Plant AL, Gueguetchkeri M, Yap W. *Biophys. J* 1994;67:1126. [PubMed: 7811924]
40. Plant AL, Brigham-Burke M, Petrella EC, O'Shannessy DJ. *Anal. Biochem* 1995;226:342. [PubMed: 7793636]
41. Meuse CW, Krueger S, Majkrzak CF, Dura JA, Fu J, Connor JT, Plant AL. *Biophys. J* 1998;74:1388. [PubMed: 9512035]
42. Meuse CW, Niaura G, Lewis ML, Plant AL. *Langmuir* 1998;14:1604.
43. Plant AL. *Langmuir* 1999;15:5128.
44. Lahiri J, Kalal P, Frutos AG, Jonas SJ, Schaeffler R. *Langmuir* 2000;16:7805.
45. Lingler S, Rubinstein I, Knoll W, Offenhausser A. *Langmuir* 1997;13:7085.
46. Wang XB, Huang Y, Wang X, Becker FF, Gascoyne PR. *Biophys. J* 1997;72:1887. [PubMed: 9083692]
47. Gascoyne P, Pethig R, Satayavivad J, Becker FF, Ruchirawat M. *Biochim. Biophys. Acta* 1997;1323:240. [PubMed: 9042346]
48. Eylar EH, Madoff MA, Brody OV, Oncley JL. *J. Biol. Chem* 1962;237:1992. [PubMed: 13891108]
49. Seaman GVF, Uhlenbruck G. *Arch. Biochem. Biophys* 1963;100:493. [PubMed: 13987517]
50. Chan KL, Gascoyne PR, Becker FF, Pethig R. *Biochim. Biophys. Acta* 1997;1349:182. [PubMed: 9421190]

51. Yang J, Huang Y, Wang X, Wang XB, Becker FF, Gascoyne PRC. *Biophys. J* 1999;76:3307. [PubMed: 10354456]
52. [www.dynalparticles.com](http://www.dynalparticles.com)
53. Petrache HI, Dodd SW, Brown MF. *Biophys. J* 2000;79:3172. [PubMed: 11106622]
54. Benz R, Frohlich O, Lauger P, Montal M. *Biochim. Biophys. Acta* 1975;394:323. [PubMed: 1131368]
55. Chidsey CED, Loiacono DN. *Langmuir* 1990;6:682.
56. Fenter P, Eisenberger P, Liang KS. *Phys. Rev. Lett* 1993;70:2447. [PubMed: 10053564]
57. Bryant MA, Pemberton JE. *J. Am. Chem. Soc* 1991;113:3629.
58. Buranda T, Huang J, Perez-Luna VH, Schreyer B, Sklar LA, Lopez GP. *Anal. Chem* 2002;74:1149. [PubMed: 11924977]
59. Sato K, Tokeshi M, Otake T, Kimura H, Ooi T, Nakao M, Kitamori T. *Anal. Chem* 2000;72:1144. [PubMed: 10740851]
60. Andersson H, van der Wijngaart W, Enoksson P, Stemme G. *Sens. Actuators, B* 2000;67:203.
61. Andersson H, van der Wijngaart W, Stemme G. *Electrophoresis* 2001;22:249. [PubMed: 11288892]
62. Andersson H, Jonsson C, Moberg C, Stemme G. *Electrophoresis* 2001;22:3876. [PubMed: 11700716]
63. Edmiston PL, Saavedra SS. *J. Am. Chem. Soc* 1998;120:1665.
64. Mao H, Yang T, Cremer PS. *Anal. Chem* 2002;74:379. [PubMed: 11811412]
65. Bamdad C. *Biophys. J* 1998;75:1997. [PubMed: 9746541]

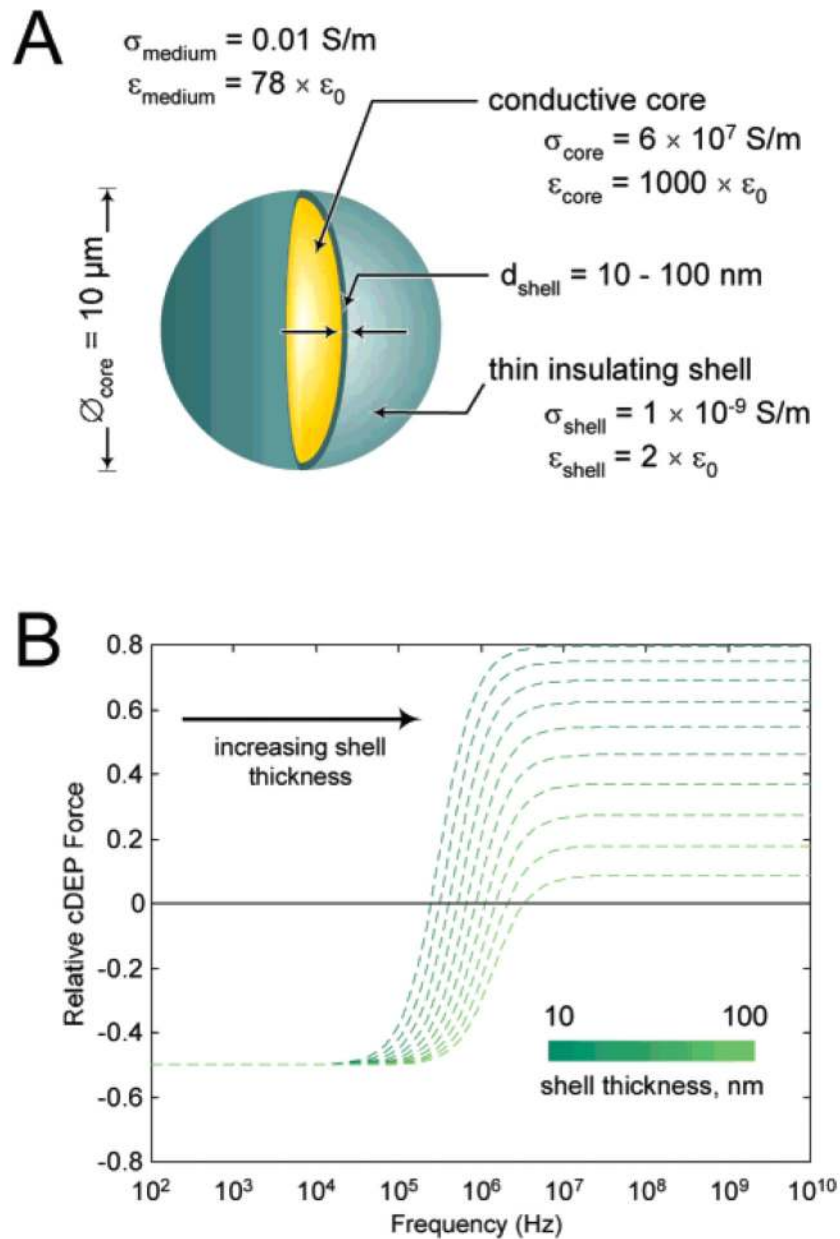


**Figure 1.**

(A) Structure of an engineered microsphere comprising a highly conductive core surrounded by a thin insulating layer. Such biomimetic particles were designed to have specified dielectric properties and dielectrophoretic behaviors. (B) The frequency-dependent cDEP response was modeled (see text) for such particles having different specified dielectric properties. In this example, the thickness of the insulating shell ( $d_{\text{shell}}$ ) was varied from 10 to 100 nm. At the crossover frequency,  $f_c$ , the relative cDEP force acting on the microsphere is zero. At frequencies below  $f_c$ , the particle experiences negative dielectrophoresis, and at frequencies above  $f_c$ , the particle experiences positive dielectrophoresis. Notice that the DEP crossover frequency is predicted to increase with increasing shell thickness. Similar modeling can be used to predict the effects of altering other parameters of the microsphere structure.

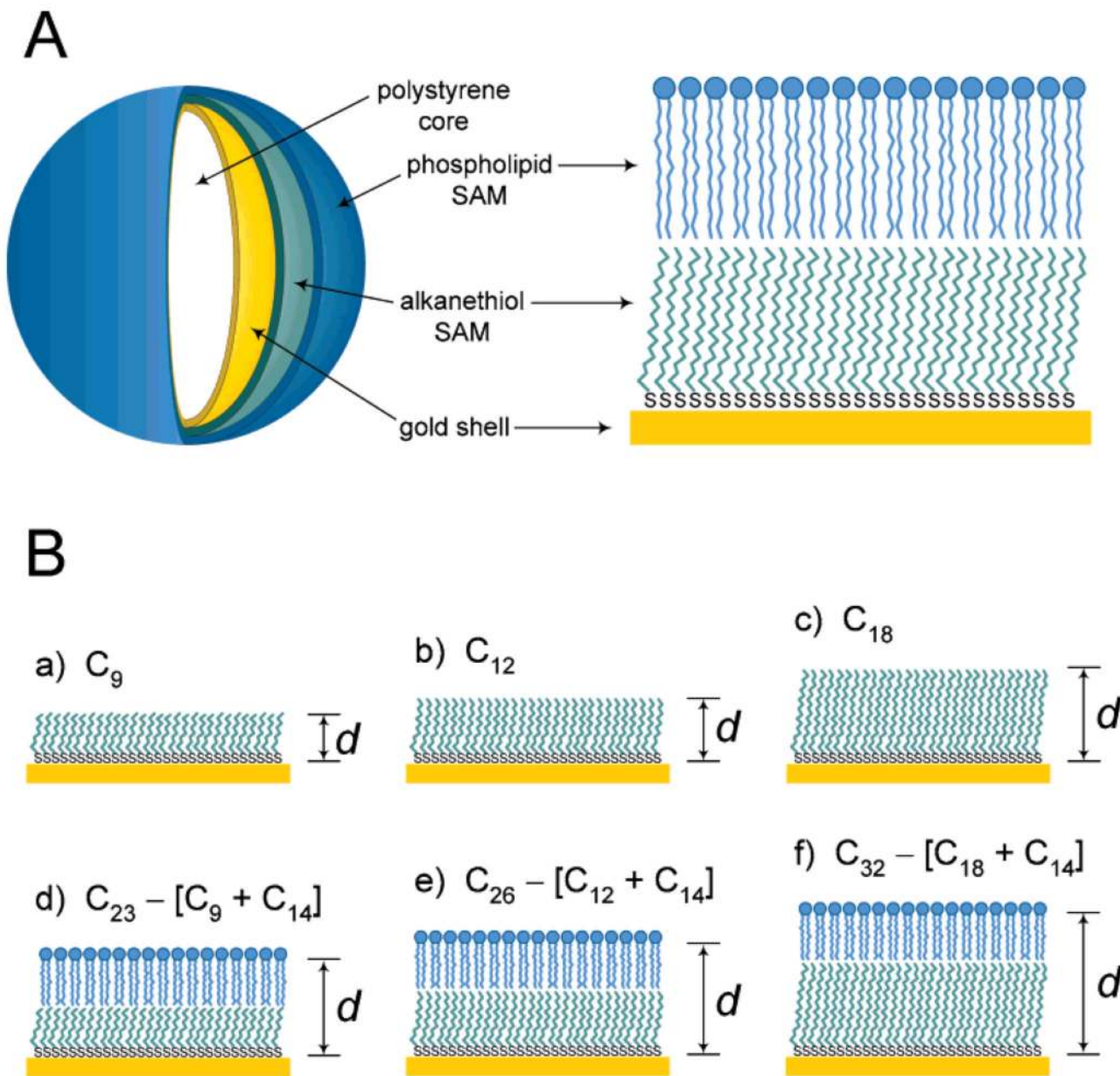


**Figure 2.** (A) Engineered microsphere architecture used in the present study. The depicted microsphere comprises a gold-coated polystyrene core particle surrounded by a SAM of alkanethiolate with an optional self-assembled outer layer of phospholipid. The thickness of the insulating layer, and therefore the corresponding dielectric properties of the particle, can be adjusted by changing the length of the hydrocarbon chains in the alkanethiol and phospholipid that are used to form the self-assembled monolayers. (B) Panel of different engineered dielectric microsphere types. Microspheres were coated with insulating shells of six different compositions: (a) a  $C_9$  alkanethiol SAM shell; (b) a  $C_{12}$  alkanethiol SAM shell; (c) a  $C_{18}$  alkanethiol SAM shell; (d) a  $C_9$  alkanethiol SAM plus a  $C_{14}$  phospholipid SAM to yield a  $C_{23}$  shell; (e) a  $C_{12}$  alkanethiol SAM plus a  $C_{14}$  phospholipid SAM to yield a  $C_{26}$  shell; (f) a  $C_{18}$  alkanethiol SAM plus a  $C_{14}$  phospholipid SAM to yield a  $C_{32}$  shell.

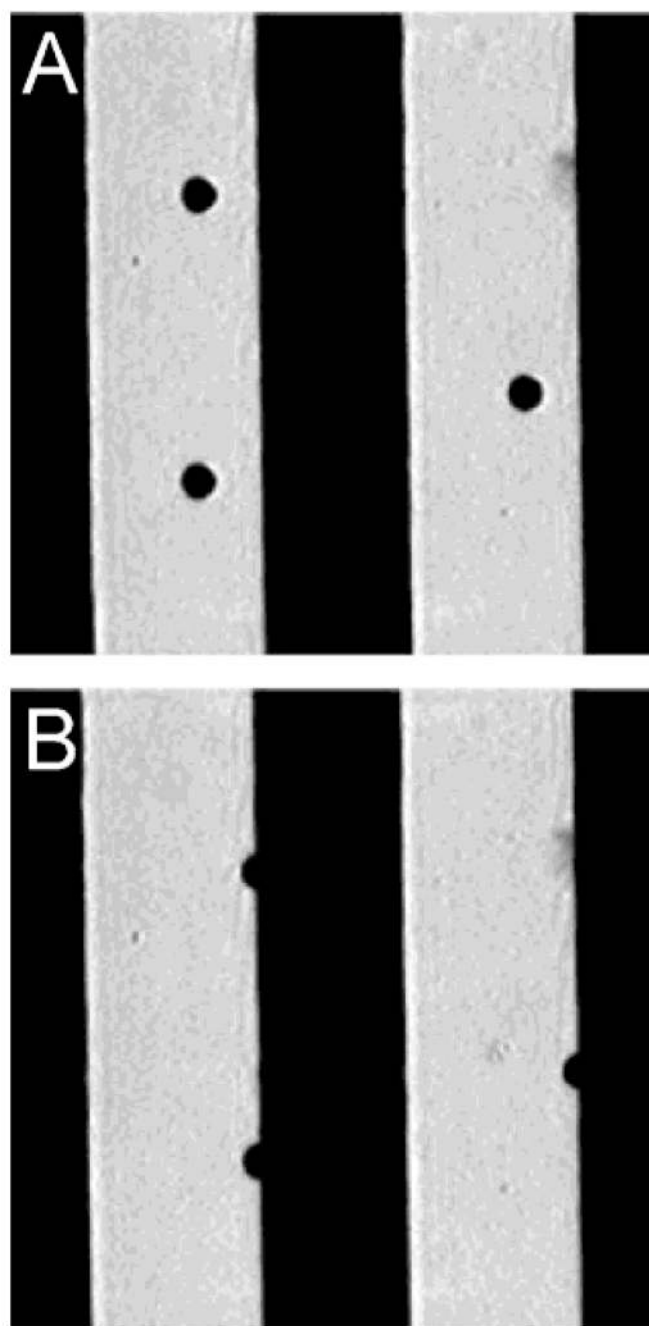


**Figure 3.** Dielectrophoretic manipulation of engineered microspheres.  $C_{32}$  ( $C_{18} + C_{14}$ ) microspheres were suspended in an aqueous medium ( $220 \mu\text{S}/\text{cm}$  conductivity) above a parallel gold-on-glass electrode array as described in the Experimental Section. An inhomogeneous fringing electric field, normal to the electrode plane, is generated at the edges of the  $0.35 \mu\text{m}$  thick gold electrodes. The metallized electrode traces appear as dark bands; microspheres can be observed in the open glass areas between the electrodes. (A) At  $10 \text{ kHz}$  ( $3 \text{ Vp-p}$ ), negative DEP forces direct particles to the field minima between electrode pairs. (B) At  $70 \text{ kHz}$ , positive DEP forces direct particles to the field maxima at the electrode edges.

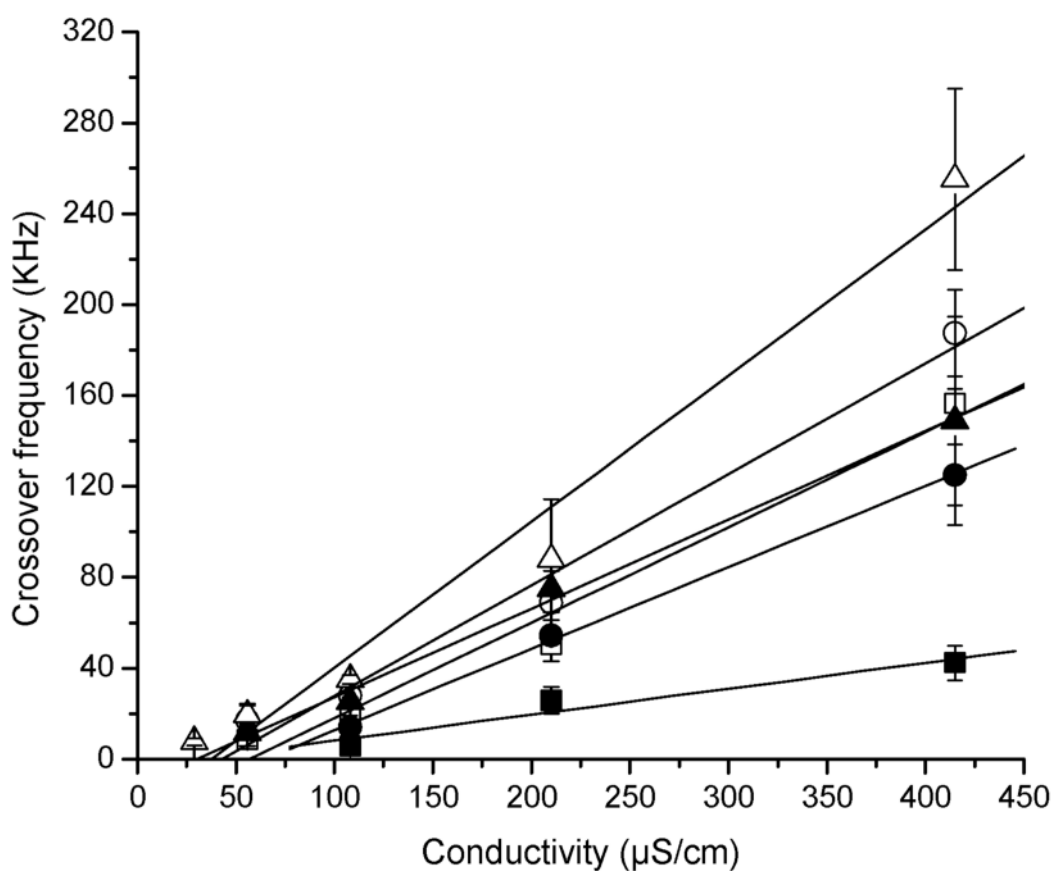


**Figure 4.**

Experimentally determined dependence of the crossover frequency on the insulating shell composition. The dielectric crossover frequency was determined for each microsphere type as a function of the electrical conductivity of the suspending medium as described in the Experimental Section: (■) C<sub>9</sub> shell; (●) C<sub>12</sub> shell; (▲) C<sub>18</sub> shell; (□) C<sub>23</sub> (C<sub>9</sub> + C<sub>14</sub>) shell; (○) C<sub>26</sub> (C<sub>12</sub> + C<sub>14</sub>) shell; (△) C<sub>32</sub> (C<sub>18</sub> + C<sub>14</sub>) shell. Each point represents the mean and standard deviation for five individual microspheres.



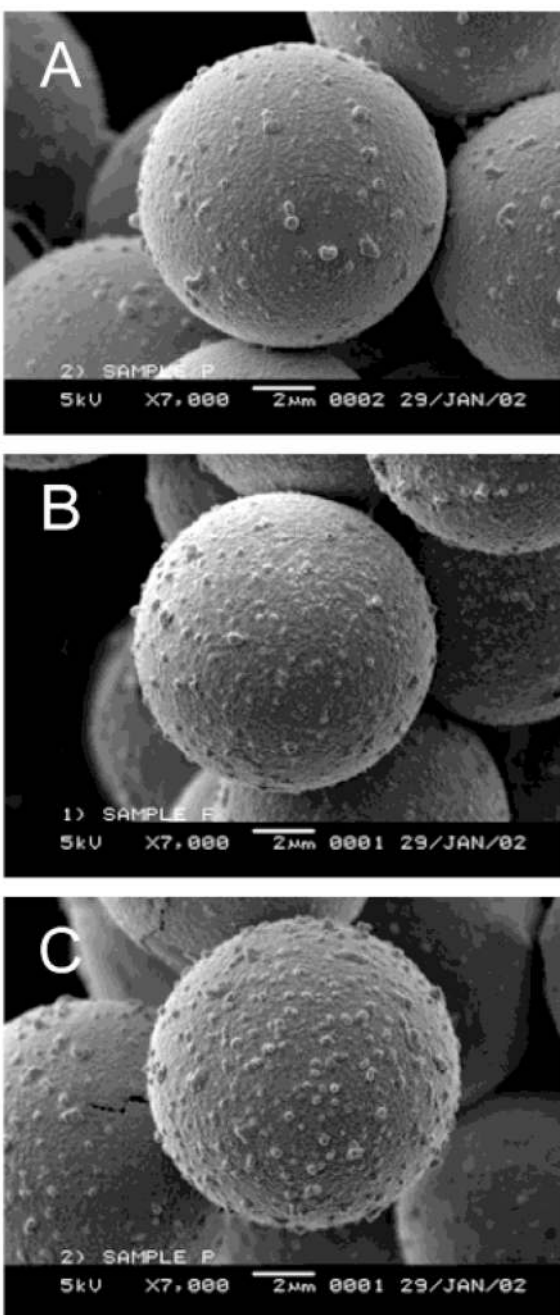


**Figure 5.** SEM photos of gold-coated microsphere core particles. These images were obtained using a JEOL JSM-5900 scanning electron microscope. Note the presence of surface roughness from the gold-coating process and the variability in surface area for the three example microspheres from the same lot (shown in panels A, B, and C).

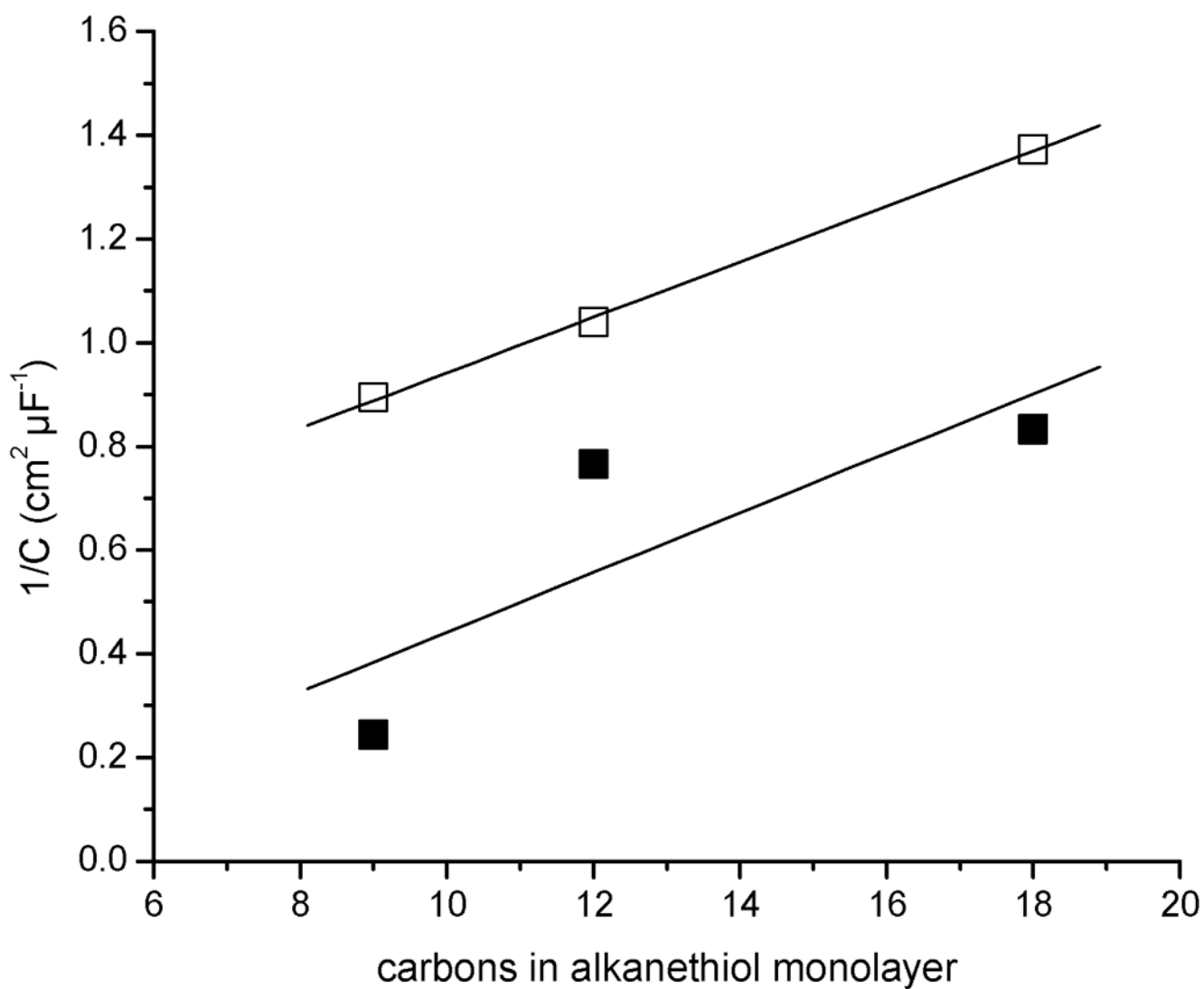


**Figure 6.** Insulating shell characteristics as a function of layer composition. Crossover frequency values and eq 5 (see text) were used to calculate the specific membrane capacitance for microspheres coated with either (■) an alkanethiol self-assembled monolayer or (□) an alkanethiol SAM with an additional DMPC phospholipid layer to yield a HBM.

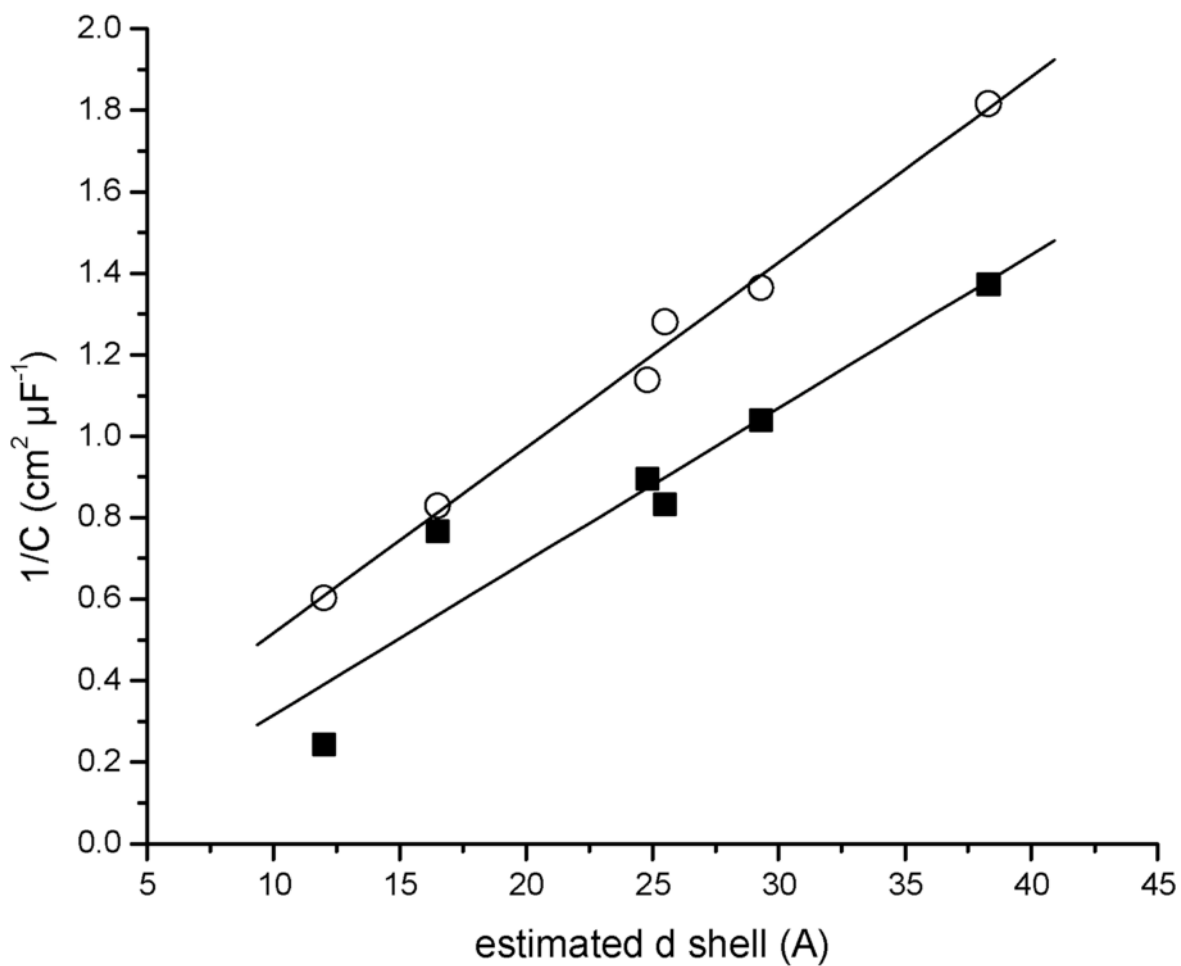


**Figure 7.** Dependence of the specific membrane capacitance on insulating shell thickness. Specific membrane capacitance values are as follows: (■) experimental values derived from dielectrophoretic crossover frequency data; (○) theoretical values calculated using basic capacitance theory (eq 6 and eq 8, see text).